AGU PUBLICATIONS

Geophysical Research Letters

RESEARCH LETTER

10.1002/2014GL062780

I. Reiweger and J. Gaume equally contributed to this work.
doi:10.1002/2014GL062780.

Key Points:
- A new mixed-mode failure criterion for weak snowpack layers
- A Mohr-Coulomb-Cap model is able to reproduce our experiments on snow failure
- For typical avalanche slopes (>30 degrees), the Mohr-Coulomb criterion is sufficient

Correspondence to:
I. Reiweger and J. Gaume,
reiweger@slf.ch;
gaume@slf.ch

Citation:
Reiweger, I., J. Gaume, and J. Schweizer (2015), A new mixed-mode failure criterion for weak snowpack layers, *Geophys. Res. Lett.*, *42*, 1427–1432, doi:10.1002/2014GL062780.

Received 8 DEC 2014
Accepted 26 JAN 2015
Accepted article online 29 JAN 2015
Published online 9 MAR 2015

A new mixed-mode failure criterion for weak snowpack layers

I. Reiweger[1], J. Gaume[1], and J. Schweizer[1]

[1]WSL Institute for Snow and Avalanche Research SLF, Davos, Switzerland

Abstract The failure of a weak snow layer is the first in a series of processes involved in dry-snow slab avalanche release. The nature of the initial failure within the weak layer is not yet fully understood but widely debated. The knowledge of the failure criterion is essential for developing avalanche release models and hence for avalanche hazard assessment. Yet different release models assume contradictory criteria as input parameters. We analyzed loading experiments on snow failure performed in a cold laboratory with samples containing a persistent weak snow layer of either faceted crystal, depth hoar, or buried surface hoar. The failure behavior of these layers can be described well with a modified Mohr-Coulomb model accounting for the possible compressive failure of snow. We consequently propose a new mixed-mode shear-compression failure criterion that can be used in avalanche release models.

1. Introduction

A dry-snow slab avalanche (Figure 1a) involves the release of a layer of cohesive snow—the slab—that slides down the mountain, breaking into pieces during movement. Slab avalanches cause most of the property damage and fatalities related to avalanche activity [*McClung and Schaerer*, 2006]. Such avalanches originate due to damage leading to a localized initial failure in a weak snow layer (Figure 1b) beneath the cohesive slab followed by the onset of rapid crack propagation within the weak layer [*McClung*, 1979; *Schweizer et al.*, 2003]. Our present understanding of dry-snow slab avalanche release is still incomplete with regard to the very first process, i.e., failure initiation, mainly due the complex microstructure and the highly porous character of weak snowpack layers. Recent field experiments have highlighted the possible structural collapse of the weak layer [*van Herwijnen et al.*, 2010] resulting in the typical "whumpf" sound. Hence, the question of the origin of the initial failure, whether it is in shear, as assumed for years, or compression, has been raised and is still a matter of debate. However, as the damage in the weak layer is due to bond breaking at the microscopic scale, the stress distribution due to mixed-mode loading on a slope is likely to be highly complex due to the nonuniform distribution of snow grains in the weak layer [*Schweizer and Jamieson*, 2008]. Most current avalanche release models assume pure shear or Mohr-Coulomb failure criteria [*Chiaia et al.*, 2008; *Fyffe and Zaiser*, 2007; *Gaume et al.*, 2014b; *Schweizer et al.*, 2006]. However, such criteria are incomplete since they do not account for the possible compressive failure of the most common weak snow layers consisting of either faceted crystals (depth hoar) or buried surface hoar [*Schweizer and Jamieson*, 2001]. On the other hand, the anticrack model developed by *Heierli et al.* [2008] takes into account the effect of slab bending induced by the collapse of the weak layer to assess the stability of a preexisting crack. However, it is not suitable to address the issue of the very initial failure in the weak layer. Furthermore, none of the latter models accounts for the important rate dependency of snow failure.

To address this controversial issue of failure initiation, we developed a mixed-mode shear-compression failure criterion for weak snow layers relevant for avalanche release. The model was calibrated on a unique set of loading experiments of sandwich specimens (Figure 2) including a natural or artificial weak snow layer [*Reiweger and Schweizer*, 2010, 2013]. The snow samples were loaded at different loading rates and different slope angles until catastrophic failure.

2. Methods

We analyzed data from loading experiments with snow samples containing various kinds of weak layers. The samples were loaded with an increasing force until catastrophic failure at different "slope" angles, i.e., different proportions of shear to normal load. The loading rates ranged from 1 to 440 Pa s^{-1}, which approximately corresponds to natural (wind) loading of a snow slope and artificial (skier) loading, respectively. Slope angles ranged from 0° (no tilting) to 35°. The weak layers consisted either of surface hoar

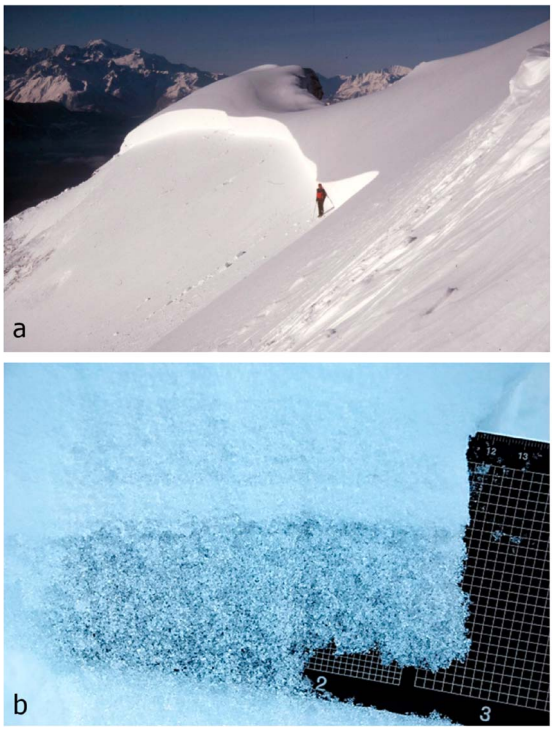

Figure 1. (a) Crown fracture of a dry-snow slab avalanche in La Sionne, Switzerland ©SLF. (b) Depth hoar weak layer.

(crystal size: 5 mm, hand hardness: very soft) or of faceted crystals including some depth hoar crystals (crystal size: 1 mm, hand hardness: very soft). The loading apparatus (Figure 2) is described in detail in *Reiweger et al.* [2009a] and *Reiweger et al.* [2010]. Most of the experimental data have been introduced by *Reiweger and Schweizer* [2010, 2013]. For the present analysis we merged the data from all experiments so that the data set now includes a total of 39 experiments. The slope angles, loading rates, and total strengths of the different samples used for the experiments are summarized in Table 1.

3. Experimental Results

The failure criterion is the envelope of the shear stress τ versus the normal stress σ at the time of the catastrophic failure. It separates stress states where the material remains intact and stress states which lead to the failure of the material. The data from all experiments with different weak snow layers and for different loading rates were represented in the $\sigma - \tau$−plane in Figure 3. For low values of the normal stress σ (< 2.3 kPa), corresponding to high values of the slope angle, the shear stress τ increases almost linearly with increasing normal stress for all types of weak layers and for all loading rates. Then, for high loading rates ("fast" experiments) and for low values of the slope angle, the shear stress starts to decrease with increasing normal stress. The transition occurs for $\sigma \approx 2.4$ kPa, corresponding to a slope angle $\theta \approx 23°$. The same transition occurs for low loading rates ("slow" experiments) but for a higher value of the normal stress $\sigma \approx 4.5$ kPa corresponding to a slope angle of $\theta \approx 21.5°$. Furthermore, the extremely fragile (soft) surface hoar samples that were loaded "slowly," at loading rates of $\approx 2\,\mathrm{Pa\,s^{-1}}$ exhibited ductile behavior, while in fast experiments, for loading rates of $\approx 20\,\mathrm{Pa\,s^{-1}}$, brittle behavior was observed. The samples containing weak layers consisting of mainly faceted crystals exhibited ductile behavior at rates of $\approx 40\,\mathrm{Pa\,s^{-1}}$ (slow experiments) and brittle behavior at loading rates of $\approx 200\,\mathrm{Pa\,s^{-1}}$ (fast experiments). All the samples, for different loading rates and slope angles, were weaker in shear than in compression as τ was always lower than σ at the time of catastrophic failure.

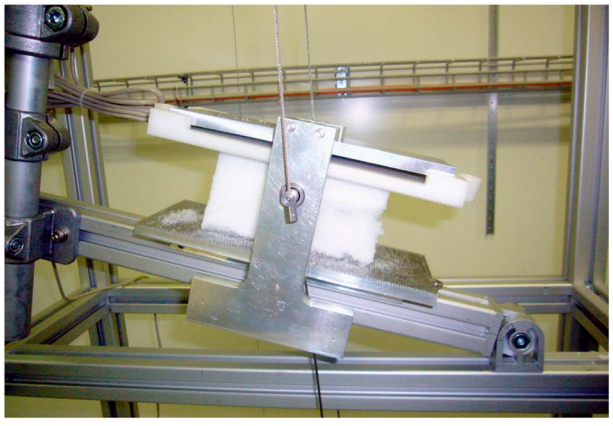

Figure 2. Snow sample including a weak snow layer in the mixed-mode loading apparatus.

4. Model Development: Failure Criterion

Analyzing the experimental results of all our loading experiments shown in Figure 3, we propose a modified Mohr-Coulomb criterion with a cap model [*Resende and Martin*, 1985; *Han et al.*, 2008] well suited to fit all our data (MCC: Mohr-Coulomb-Cap model). For high values of the slope angle and thus small compressive stresses the conventional Mohr-Coulomb criterion

$$\tau_{MC} = c + \sigma \tan\phi = (\sigma_t + \sigma)\tan\phi \quad (1)$$

Table 1. Experimental Results for Slope Angle θ, Loading Rate, Total Strength σ_f (Stress at Fracture), and Number of Experiments N_{exp}

Samples	Slope Angle θ (deg)	Loading Rate (Pa s^{-1})	Strength σ_f (kPa)	N_{exp}
SH_{slow}	15–25	1–3.3	0.5–7	4
SH_{fast}	15–25	12–21	0.26–2.6	6
FCN_{slow}	0–35	9–42	1.6–6	9
FCN_{fast}	0–35	84–444	0.7–2.7	8
FCA_{slow}	10–30	60	0.5–5.3	6
FCA_{fast}	10–30	150–444	1.1–2.6	6

allows to reproduce our data. The shear stress at failure τ_{MC} is a function of the normal stress σ, while c denotes the cohesion (shear strength at zero normal stress, $\theta = 90°$), ϕ the angle of internal friction, and σ_t the tensile strength (found for a pure tension test, $\theta = 180°$). However, in order to model the failure observed for low values of the slope angle which are not consistent with the classical MC model, we define the equation of the cap for our failure criterion

$$\tau_{cap} = b\sqrt{1 - \frac{(\sigma + \sigma_t)^2}{(\sigma_c + \sigma_t)^2}}, \tag{2}$$

with

$$b = \sqrt{\frac{(\sigma_c + \sigma_t)^2}{(\sigma_c + \sigma_t)^2 - \left(\frac{K}{\tan\phi}\right)^2}}, \tag{3}$$

where σ_c is the compressive strength (found in a pure compression test, $\theta = 0°$) and K the maximum shear strength value (shear strength at the transition between the MC and the cap models).

From the failure envelope fitted to our experimental data, we found a range of possible angles of internal friction between 12 and 28° represented by the shaded domain in Figure 3 with an average value of 20°. This range allows reproducing fast and slow experiments for slope angles typically higher than the internal friction angle. The tensile strength σ_t is equal to 0.4 kPa and the cohesion to 0.17 kPa approximately.

However, the order of magnitude of the shear stress which marks the transition between Mohr-Coulomb and Cap behavior depends on the rate at which the snow samples were loaded (Figure 3). A slower loading rate leads to a higher failure stress ($K^{fast} \approx 1$ kPa, $K^{slow} \approx 1.8$ kPa). Hence, the compressive strength σ_c is about 2.6 kPa for fast and 5.7 kPa for slow experiments.

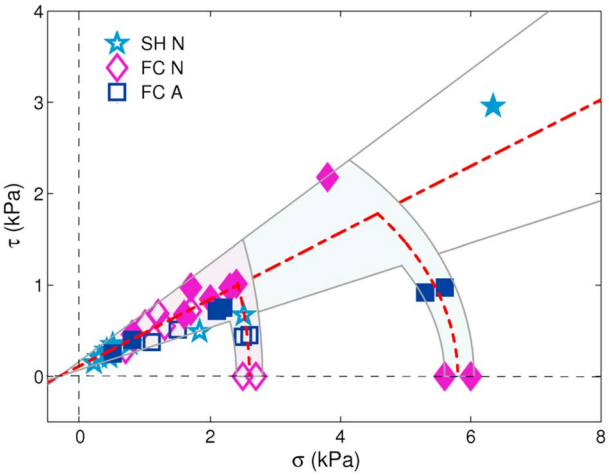

Figure 3. Failure criterion, i.e., envelope of the shear stress versus normal stress at failure for experimental data from loading experiments with three different kinds of weak snow layers, natural surface hoar (SH N), natural faceted and depth hoar crystals (FCN), and artificial faceted crystals (FCA). The full symbols represent slow and the empty symbols fast for experiments with low and high loading rates, respectively.

A schema of our model is represented in Figure 4 where shear stress τ is plotted versus normal stress σ. The model incorporates tensile strength σ_t, compressive strength σ_c, cohesion c, slope angle θ, and friction angle ϕ. The angles θ_t^{fast} and θ_t^{slow} define the transition angles where Mohr-Coulomb changes to Cap behavior.

The influence of the slope angle on the total strength of the weak layer according to our MCC model is shown in Figure 5. The total strength corresponds to the value of $\sigma_f = \sqrt{\tau^2 + \sigma^2}$ at the time of failure.

The total strength of the weak layer decreases with increasing slope angle. Initially, the decrease is minor as long as the total strength follows the Cap behavior (red solid line in Figure 5). For slope angles

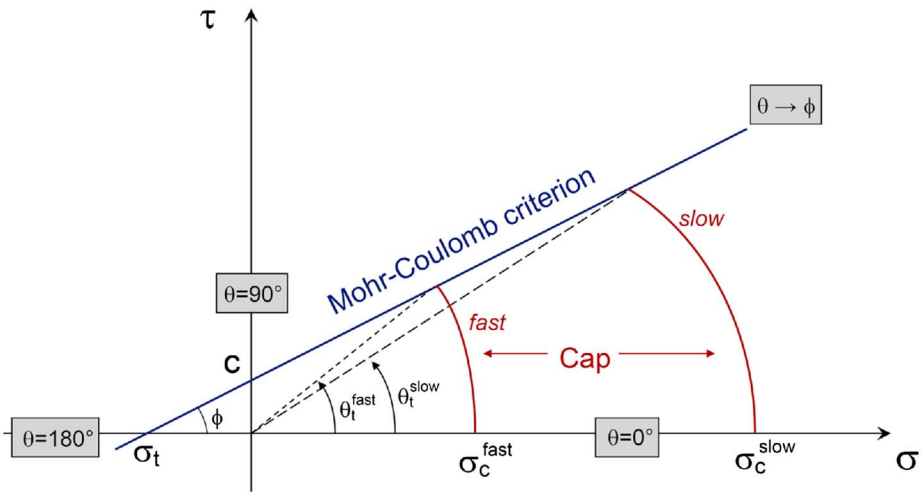

Figure 4. Schematic representation of our failure criterion.

larger than $\theta_t^{slow} = 21.5°$ and $\theta_t^{fast} = 23°$ the total stress follows the Mohr-Coulomb behavior (blue solid line in Figure 5) and hence sharply decreases with increasing slope angle for slow and fast experiments, respectively.

5. Discussion

We analyzed experiments using a load-controlled test apparatus to characterize the failure behavior of weak snowpack layers. The results of our experiments showed that for high values of the slope angle, i.e., for low values of the normal stress, the shear stress at failure increases with increasing normal stress. However, due to the collapsible nature of the high-porosity material snow, we also found failure in case of pure compressive loading, i.e., without any shear stress, provided the compressive stress was sufficiently large. This behavior is quite typical for other (porous) granular materials such as sand or clay [*Dimaggio and Sandler*, 1971; *Resende and Martin*, 1985].

We developed a mixed-mode shear-compression failure criterion based on the Mohr-Coulomb-Cap model that reproduced our experiments. The angle of internal friction that we found $\phi \approx 20°$ is in agreement with the recent findings of [*Podolskiy et al.*, 2014a] who found friction angles typically between 15 and 30° and with the study of *Roch* [1966] who found an angle of internal friction of about 22°. This friction angle value, however, is lower than the dry (or crack face) friction which is typically around 30° [*van Herwijnen and Heierli*, 2009]. The latter value is generally used in avalanche release models using the MC criterion [*Gaume et al.*, 2013, 2014a, 2014b; *Podolskiy et al.*, 2014b] and is thus slightly too high.

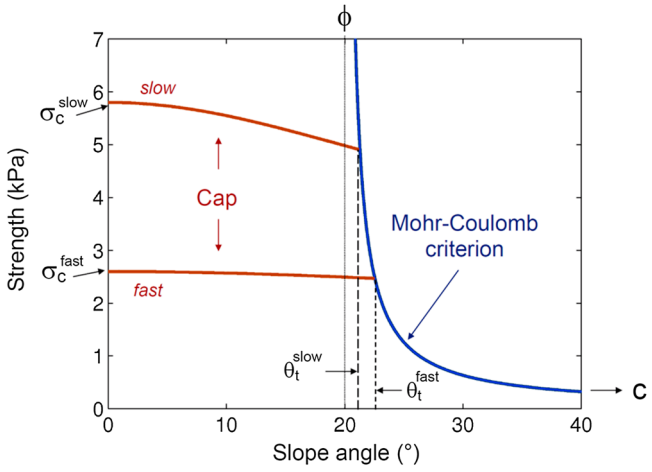

Figure 5. Total strength of the weak layer as a function of the slope angle.

The rate dependency of the transition point from the Mohr-Coulomb to the cap behavior is in accordance with the fact that the snow failure behavior is rate dependent in general [e.g., *Schweizer*, 1998] but in particular for weak snow layers [*Reiweger and Schweizer*, 2010, 2013]. These studies showed a transition from ductile to brittle behavior with a higher failure stress for the ductile case with increasing strain rate. The loading rates needed to achieve brittle behavior were higher for the moderately soft

faceted samples than for the extremely soft surface hoar samples. We assume that this is due to the fact that deformation at a given stress is inversely proportional to elastic modulus. The ductile to brittle transition itself can be explained by the competition between different time scales corresponding to the relatively slow sintering (healing) of broken bonds and the fast process of bond breaking [*Reiweger et al.*, 2009b]. Nevertheless, for both fast and slow experiments, this transition appears for a slope angle lower than 30°. Hence, for typical avalanche slopes, it might be sufficient to implement the MC criterion into slab avalanche release models.

Recently *Birkeland et al.* [2014] performed a field study on the effect of slope angle on stability test results using the compression test (CT). The CT provides a measure of failure initiation propensity. They found that the test results were almost independent of slope angle; in one out of three data sets a slight increase with increasing slope angle was observed. Our results (Figure 5) suggest that similar strength might be expected on slopes between 0 and about 23°, but weak layer strength should decrease for higher values of the slope angle. As any stability test result is influenced by weak layer as well as slab properties [*Schweizer and Jamieson*, 2010], it is not fully clear what our results mean in terms of CT score, unless slab properties and the type of loading would not change with increasing slope angle. To assess the effect of slope angle on slab and weak layer properties, we suggest to perform snow micropenetrometer measurements as the relevant properties can now be derived [*Reuter et al.*, 2014; *Schweizer and Reuter*, 2015].

Finally, the experimental results we show as well as the proposed model suggest that the recent debate, namely, whether the initial failure occurs in shear or compression [*Schweizer and Jamieson*, 2008] is irrelevant. This debate was raised by new theoretical ideas [*Heierli et al.*, 2008] and experimental evidence [*van Herwijnen et al.*, 2010] suggesting that the structural collapse of the weak layer is required for crack propagation. However, these recent findings assume a preexisting crack in the weak layer and thus only concern crack propagation but not the initiation of the failure. The experiments we conducted on failure initiation (and hence crack formation) suggest that weak layer collapse is a secondary process and a consequence of the damage and eventually the failure in the weak layer [*Reiweger and Schweizer*, 2013]. Failure initiation itself is presumably the result of bond breaking at the microscopic scale leading to a complex relation between shear and normal stresses and thus a mixed-mode failure criterion.

6. Conclusions

The analysis of a unique set of experiments on the failure of weak snow layers allowed us to describe for the first time the failure criterion of different types of weak layers loaded at different rates. This failure criterion was described using a modified Mohr-Coulomb model, namely, the Mohr-Coulomb-Cap model which reflects the mixed-mode shear-compression failure of snow and which was able to reproduce all our experiments. Besides, it was shown that the simple Mohr-Coulomb criterion is able to appropriately represent failure of a weak snow layer consisting of either faceted/depth hoar crystals or surface hoar crystals for slope angles higher than about 23°. Hence, the Mohr-Coulomb criterion seems be sufficient, in practice, to model weak layer failure for avalanche slopes that are typically steeper than 30°.

However, for comprehensively modeling dry-snow slab avalanche release not only failure initiation but also crack propagation needs to be considered. Failure initiation in the weak layer includes damage acceleration and localization and results in an initial crack. This crack can propagate if it exceeds a critical size or if the load exceeds a critical value. Hence, in the future, the coupling between the proposed failure initiation criterion and a suitable crack propagation model [*Heierli et al.*, 2008; *Chiaia et al.*, 2008; *Gaume et al.*, 2014b] may eventually provide a comprehensive model of slab avalanche release.

Acknowledgments

Document data are available on request by sending an email to J. Gaume at gaume@slf.ch. J. Gaume was supported by a Swiss Government Excellence Scholarship and is grateful to the State Secretariat for Education, Research and Innovation SERI of the Swiss Government. We thank K. Birkeland and one anonymous reviewer for their insightful and constructive comments.

The Editor thanks Karl Birkeland and an anonymous reviewer for their assistance in evaluating this paper.

References

Birkeland, K. W., E. Bair, and D. Chabot (2014), The effect of changing slope angles on compression test results, in *Proceedings of the International Snow Science Workshop 2014, Banff, Alberta*, edited by P. Haegeli, pp. 746–751, Banff, Alberta, Canada, 29 Sept.-3 Oct.

Chiaia, B., P. Cornetti, and B. Frigo (2008), Triggering of dry snow slab avalanches: Stress versus fracture mechanical approach, *Cold Reg. Sci. Technol.*, *53*, 170–178.

Dimaggio, F. L., and I. S. Sandler (1971), Material model for granular soils, *J. Eng. Mech. Div.*, *97*(3), 935–950.

Fyffe, B., and M. Zaiser (2007), Interplay of basal shear fracture and slab rupture in slab avalanche release, *Cold Reg. Sci. Technol.*, *49*, 26–38.

Gaume, J., G. Chambon, N. Eckert, and M. Naaim (2013), Influence of weak-layer heterogeneity on snow slab avalanche release: Application to the evaluation of avalanche release depths, *J. Glaciol.*, *59*(215), 423–437.

Gaume, J., G. Chambon, N. Eckert, M. Naaim, and J. Schweizer (2014a), Influence of weak layer heterogeneity and slab properties on slab tensile failure propensity and avalanche release area, *Cryosphere Discuss.*, *8*(6), 6033–6057.

Gaume, J., J. Schweizer, A. van Herwijnen, G. Chambon, B. Reuter, N. Eckert, and M. Naaim (2014b), Evaluation of slope stability with respect to snowpack spatial variability, *J. Geophys. Res. Earth Surf.*, *119*, 1783–1789, doi:10.1002/2014JF003193.

Han, L., J. Elliott, A. Bentham, A. Mills, G. Amidon, and B. Hancock (2008), A modified drucker-prager cap model for die compaction simulation of pharmaceutical powders, *Int. J. Solids Struct.*, *45*(10), 3088–3106.

Heierli, J., P. Gumbsch, and M. Zaiser (2008), Anticrack nucleation as triggering mechanism for snow slab avalanches, *Science*, *321*, 240–243.

McClung, D. (1979), Shear fracture precipitated by strain softening as a mechanism of dry slab avalanche release, *J. Geophys. Res.*, *84*(B7), 3519–3526.

McClung, D., and P. Schaerer (2006), *The Avalanche Handbook*, Mountaineers, Seattle, Wash.

Podolskiy, E., M. Barbero, F. Barpi, G. Chambon, M. Borri-Brunetto, O. Pallara, B. Frigo, B. Chiaia, and M. Naaim (2014a), Healing of snow surface-to-surface contacts by isothermal sintering, *Cryosphere Discuss.*, *8*(3), 2465–2490.

Podolskiy, E., G. Chambon, M. Naaim, and J. Gaume (2014b), Evaluating snow weak-layer rupture parameters through inverse finite element modeling of shaking-platform experiments, *Nat. Hazards Earth Syst. Sci. Discuss.*, *2*(7), 4525–4580.

Reiweger, I., and J. Schweizer (2010), Failure of a layer of buried surface hoar, *Geophys. Res. Lett.*, *37*, L24501, doi:10.1029/2010GL045433.

Reiweger, I., and J. Schweizer (2013), Weak layer fracture: Facets and depth hoar, *Cryosphere Discuss.*, *7*, 1907–1925.

Reiweger, I., R. Ernst, J. Schweizer, and J. Dual (2009a), Force-controlled shear experiments with snow samples, in *Proceedings of the International Snow Science Workshop ISSW, Davos, Switzerland, 27 September - 2 October 2009*, edited by J. Schweizer and A. van Herwijnen, pp. 120–123, Swiss Federal Institute for Forest, Snow and Landscape Research WSL, Birmensdorf, Switzerland.

Reiweger, I., J. Schweizer, J. Dual, and H. Herrmann (2009b), Modelling snow failure with a fibre bundle model, *J. Glaciol.*, *55*(194), 997–1002.

Reiweger, I., J. Schweizer, R. Ernst, and J. Dual (2010), Load-controlled test apparatus for snow, *Cold Reg. Sci. Technol.*, *62*(2), 119–125.

Resende, L., and J. B. Martin (1985), Formulation of drucker-prager cap model, *J. Eng. Mech.*, *111*(7), 855–881.

Reuter, B., J. Schweizer, and A. van Herwijnen (2014), A process-based approach to estimate point snow instability, *Cryosphere Discuss.*, *8*(6), 5825–5856.

Roch, A. (1966), Les déclenchements d'avalanches, in *Symposium at Davos 1965 – Scientific Aspects of Snow and Ice Avalanches, IAHS Publication*, vol. 69, pp. 182–197, Int. Assoc. Hydrol. Sci., Wallingford, U. K.

Schweizer, J. (1998), Laboratory experiments on shear failure of snow, *Ann. Glaciol.*, *26*, 97–102.

Schweizer, J., and B. Jamieson (2008), Dry-snow slab avalanche release revisited: Shear vs. collapse?, Geophysical Research Abstracts 2008-A-10994 presented at EGU General Assembly, vol. 10.

Schweizer, J., and B. Jamieson (2010), Snowpack tests for assessing snow-slope instability, *Ann. Glaciol.*, *51*(54), 187–194.

Schweizer, J., and J. Jamieson (2001), Snow cover properties for skier triggering of avalanches, *Cold Reg. Sci. Technol.*, *33*(2), 207–221.

Schweizer, J., and B. Reuter (2015), A new index combining weak layer and slab properties for snow instability prediction, *Nat. Hazards Earth Syst. Sci.*, *15*, 109–118.

Schweizer, J., B. Jamieson, and M. Schneebeli (2003), Snow avalanche formation, *Rev. Geophys.*, *41*(4), 1016, doi:10.1029/2002RG000123.

Schweizer, J., S. Bellaire, C. Fierz, M. Lehning, and C. Pielmeier (2006), Evaluating and improving the stability predictions of the snow cover model SNOWPACK, *Cold Reg. Sci. Technol.*, *46*(1), 52–59.

van Herwijnen, A., and J. Heierli (2009), Measurement of crack-face friction in collapsed weak snow layers, *Geophys. Res. Lett.*, *36*, L23502, doi:10.1029/2009GL040389.

van Herwijnen, A., J. Schweizer, and J. Heierli (2010), Measurement of the deformation field associated with fracture propagation in weak snowpack layers, *J. Geophys. Res.*, *115*, F03042, doi:10.1029/2009JF001515.